BOREAS An international journal of Quaternary research

Ice-margin retreat and grounding-zone dynamics during initial deglaciation of the Storfjordrenna Ice Stream, western Barents Sea

CALVIN S. SHACKLETON, MONICA C. M. WINSBORROW, KARIN ANDREASSEN, RENATA G. LUCCHI AND LILJA R. BJARNADÓTTIR

BOREAS

Shackleton, C. S., Winsborrow, M. C. M., Andreassen, K., Lucchi, R. G. & Bjarnadóttir, L. R.: Ice-margin retreat and grounding-zone dynamics during initial deglaciation of the Storfjordrenna Ice Stream, western Barents Sea. *Boreas*. https://doi.org/10.1111/bor.12420. ISSN 0300-9483.

Processes occurring at the grounding zone of marine terminating ice streams are crucial to marginal stability, influencing ice discharge over the grounding-line, and thereby regulating ice-sheet mass balance. We present new marine geophysical data sets over a ~30×40 km area from a former ice-stream grounding zone in Storfjordrenna, a large cross-shelf trough in the western Barents Sea, south of Svalbard. Mapped ice-marginal landforms on the outer shelf include a large accumulation of grounding-zone deposits and a diverse population of iceberg ploughmarks. Published minimum ages of deglaciation in this region indicate that the deposits relate to the deglaciation of the Late Weichselian Storfjordrenna Ice Stream, a major outlet of the Barents Sea–Svalbard Ice Sheet. Sea-floor geomorphology records initial ice-stream retreat from the continental shelf break, and subsequent stabilization of the ice margin in outer-Storfjordrenna. Clustering of distinct iceberg ploughmark sets suggests locally diverse controls on iceberg calving, producing multi-keeled, tabular icebergs at the southern sector of the former ice margin, and deep-drafted, single-keeled icebergs in the northern sector. Retreat of the palaeo-ice stream from the continental shelf break was characterized by ice-margin break-up via large calving events, evidenced by intensive iceberg scouring on the outer shelf. The retreating ice margin stabilized in outer-Storfjordrenna, where the southern tip of Spitsbergen and underlying bedrock ridges provide lateral and basal pinning points. Ice-proximal fans on the western flank of the grounding-zone deposits document subglacial meltwater conduit and meltwater plume activity at the ice margin during deglaciation. Along the length of the former ice margin, key environmental parameters probably impacted ice-margin stability and grounding-zone deposition, and should be taken into consideration when reconstructing recent changes or predicting future changes to the margins of modern ice streams.

Calvin S. Shackleton (calvin.s.shackleton@uit.no; c.shackleton91gmail.com), Monica C. M. Winsborrow and Karin Andreassen, CAGE - Centre for Arctic Gas Hydrate, Environment and Climate, Department of Geosciences, UiT the Arctic University of Norway, Tromsø 9037, Norway; Renata G. Lucchi, OGS-Istituto Nazionale di Oceanografia e di Geofisica Sperimentale, Borgo Grotta Gigante 42C, 34010 Sgonico (TS), Italy; Lilja R. Bjarnadóttir, Geological Survey of Norway (NGU), Leiv Erikssons vei 39, Trondheim 7040, Norway; *received 30th December 2018, accepted 2nd October 2019.*

The greatest ice mass losses from both modern and palaeo-ice masses occur at ocean margins (Pritchard *et al.* 2009), where ice streams and outlet glaciers interact with the ocean at the transition between grounded and ungrounded ice: the grounding zone (Stokes & Clark 2001; Rignot *et al.* 2011). This zone is a complex area where ice, water and sediments are transferred into the marine environment via pushing, calving and melting (Powell *et al.* 1996). These processes determine the rate of ice discharge across the grounding zone (Pattyn *et al.* 2006; Schoof 2007; Katz & Worster 2010) and thus influence the stability of marine-terminating ice margins. Fluctuations may be rapidly propagated upstream, with increases in calving rates triggering ice acceleration, dynamically driven thinning, and enhanced margin retreat (Howat *et al.* 2007; Nick *et al.* 2009). The grounding zone is sensitive to internal glaciological factors, ice dynamics and geometry (Bassis & Jacobs 2013), marginal glacier hydrology and local sedimentary processes (Powell & Alley 1997), as well as external environmental factors, such as water depth, bed slope and climatic changes including atmospheric and oceanic temperatures (Moon & Joughin 2008; Sole *et al.* 2008). Elucidating the relative importance and magnitude of grounding-zone processes in different settings remains a key challenge to understanding and eventually predicting grounding-zone behaviour.

The grounding zones of palaeo-ice streams can provide important insights into long-term grounding-zone behaviour. Accumulations of glacigenic sediments create geomorphological features of distinct size, geometry, and sedimentary structure controlled by depositional, hydrological and glaciological processes occurring at marine ice margins during retreat (Powell 1990; Ottesen & Dowdeswell 2006). When ice margins remain stable at a location for some time, the build-up of sediments deposited at the grounding zone form a range of ice-marginal landforms, depending on the dominant mode of deposition. Grounding-zone wedges (GZW), ice-proximal fans, and moraines are observed across glaciated and deglaciated regions (e.g. Powell & Alley 1997; Horgan *et al.* 2013; Batchelor & Dowdeswell 2015), and are used to reconstruct the locations of, and processes occurring at, marine-terminating ice margins. Beyond the ice margin, the keels of icebergs scour sea-floor sediments to leave behind iceberg ploughmarks,

DOI 10.1111/bor.12420

which are common features in the foreground of present-day and palaeo marine-terminating outlet glaciers and ice streams (Lien *et al.* 1989; Dowdeswell *et al.* 1993; Dowdeswell & Bamber 2007; Ottesen *et al.* 2008; Livingstone *et al.* 2013; Andreassen *et al.* 2014; Dowdeswell & Hogan 2014). Here we present a detailed geomorphic study of grounding-zone landforms of the Storfjordrenna Palaeo-Ice Stream, a major outlet of the marine-based Barents Sea Ice Sheet (BSIS; Fig. 1), using high-resolution multibeam bathymetry data, shallow acoustic subsurface Chirp sub-bottom profiles, and 2D seismic profiles. This forms the basis of a reconstruction of calving and grounding-line activity during ice retreat from the continental shelf break through outer-Storfjordrenna.

Study area

The Storfjordrenna cross-shelf trough is located south of the Svalbard Archipelago in the western Barents Sea, and is up to 420 m deep, 250 km long and 125 km wide at the continental shelf break (Fig. 1A). A trough-mouth fan (TMF) extends westwards from the mouth of the trough, spanning 35 000 km^2 and comprised of 115 000 km^3 of sediments, delivered to the shelf break by ice streams operating in Storfjordrenna over multiple glaciations (Vorren & Laberg 1997). During the most recent, Late Weichselian glaciation, the Storfjordrenna Ice Stream was grounded at the continental shelf edge (Laberg & Vorren 1996; Vorren & Laberg 1997; Pedrosa *et al.* 2011; Lucchi *et al.* 2013) and had a drainage basin estimated to 60 000 km^2 (Batchelor & Dowdeswell 2014), with ice feeding in from the north over Spitsbergen, the islands of Edgeøya, Hopen, Bjørnøya, and the submerged divide along Spitsbergenbanken (Fig. 1) (Landvik *et al.* 1998; Dowdeswell *et al.* 2010, 2015; Ingólfsson & Landvik 2013). The vast drainage catchment of the Storfjordrenna Palaeo-Ice Stream spans both terrestrial and shallow to deep marine settings in the Barents Sea, and the ice stream would have been one of the largest ice catchments of the Barents Sea and Svalbard ice sheets, sensitive to climatic and oceanographic changes (Howat *et al.* 2010).

Relative glacifluvial sediment volumes observed in cores from the TMF suggest that the northern parts of the ice stream retreated from the shelf break earlier, and the southern sector remained grounded at the shelf break for longer (Pedrosa *et al.* 2011). Dated foraminifera within hemipelagic sediments in a sediment core (JM02-460-PC) taken over 60 km east from the shelf edge in

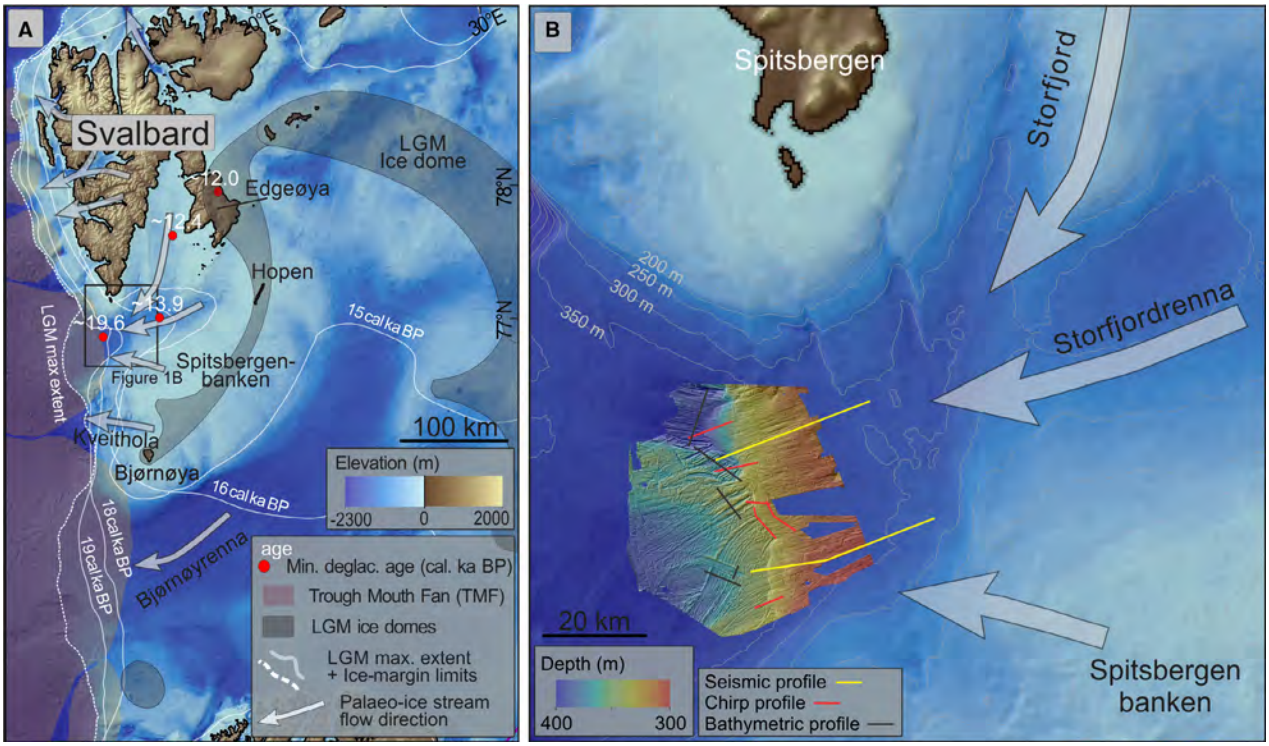

Fig. 1. A. Western Barents Sea with positions of reconstructed and modelled ice domes (Andreassen *et al.* 2008; Patton *et al.* 2017) and palaeo-ice stream flow directions (Ottesen *et al.* 2005; Dowdeswell *et al.* 2010; Pedrosa *et al.* 2011; Bjarnadóttir *et al.* 2013; Ingólfsson & Landvik 2013; Andreassen *et al.* 2014; Patton *et al.* 2015). Core locations (red dots) show minimum deglaciation age as median probability ages (cal. ka BP) within ±2σ. Full calibrated age ranges and sources are given in Table 1. The Last Glacial Maximum (LGM) ice extent maxima and most probable margin limits during retreat at 19, 18 and 15 cal. ka BP are also drawn, from the ice-sheet margin estimates presented by Hughes *et al.* (2015). Trough-mouth fan (TMF) deposits are also drawn. B. The bathymetry of outer-Storfjordrenna (Jakobsson *et al.* 2008), with the bathymetric survey presented in this study overlain and palaeo-ice stream flow directions drawn.

Table 1. Minimum ages of deglaciation surrounding Storfjordrenna, from radiocarbon AMS dating of sediment cores. Ages were recalibrated using Calib 7.1 and the MARINE13 calibration curves (see references herein).

Core/location	Uncorrected age (^{14}C years BP)	2σ range (years BP)	Median probability age (years BP)	Source	Latitude (°N)	Longitude (°S)	Material dated + sample depth (below surface)
JM02-460-PC	16 750±110	19 278–19 938	19 608	Rasmussen *et al.* (2007)	76.05	15.73	*Neogloboquadrina pachyderma* (at 460 cm) in hemipelagic sediment deposits above till.
JM09-020-GC	12 570±60	13 780–14 114	13 947	Łącka *et al.* (2015)	76.31	19.70	Bivalve shell (at 395.5 cm) beneath the upper surface of the subglacial till horizon.
JM10-10-GC	10 960±44	12 121–12 562	12 375	Rasmussen & Thomsen (2014)	Georeferenced ~77.40	~20.10	Bivalve within mixture of glaciomarine and diamictic deposits (385–386 cm).
Edgøya (Blåfjorddalen)	10 770±110	11 535–12 489	12 025	Landvik *et al.* (1992)	77.98	22.98	*Mya truncata* within silty marine sands.

outer-Storfjordrenna (Fig. 1A), indicate that retreat from the shelf edge began before *c.* 19.6 cal ka BP (Rasmussen *et al.* 2007) (Table 1 details radiocarbon dates). Core JM02-460-PC was recovered from the northern parts of the trough, suggesting that the date relates to the early retreat of the northern sector of the ice stream. Bivalve shell fragments found in a core in the inner part of the trough (Fig. 1A) suggest that central Storfjordrenna, over 150 km upstream of the shelf edge, was ice free before *c*. 13.9 cal. ka BP (Table 1; Łącka *et al.* 2015). Little is known about the dynamics of the Storfjordrenna Palaeo-Ice Stream and how it deglaciated through the outer trough. The geomorphological features presented here provide insights into the deglaciation of the Storfjordrenna Ice Stream and contribute to increasing evidence for the geomorphological signatures of marine-terminating palaeo-ice streams.

Material and methods

We utilize high-resolution swath bathymetry data for geomorphological mapping, covering 1600 km^2 and spanning water depths 300 to 400 m below sea level. Data were collected using a hull-mounted Kongsberg Simrad 30 kHz EM300 multibeam echo-sounder during two research cruises onboard the R/V 'Helmer Hanssen' in the summers of 2013 and 2014, in outer-Storfjordrenna (Fig. 1B). The bathymetry data were processed in Neptune and gridded in IVS Fledermaus v.7 to a horizontal resolution of 15×15 m. The Fledermaus software was used to visualize and interpret the data, and landforms were mapped manually in Esri ArcGIS v.10. Two 2D seismic lines were acquired during the research cruises using a Generator-Injector (GI) airgun operating in harmonic mode with total volume of 30 in^3, to generate seismic shots with a shot rate of 3 s. A hydrophone cable (16 m long, single-channel streamer) was used to record the reflected seismic signal. Seismic lines were processed in the DelphSeismic software and visualized and interpreted using Petrel v.2014.1.

Subsurface profiles were acquired in Storfjordrenna using a hull-mounted Edgetech 3300 – HM CHIRP sub-bottom sediment profiler, with 4×4 transducer array operating at 4 kW and transmitting an FM pulse, linearly swept over a full spectrum frequency range (1.5 to 9 kHz over 40 m). Data were processed, viewed and interpreted in the Kingdom Suite v.8.8 software. The velocity of sound waves is influenced by depth and rheology of the medium; however, we assume a standard velocity of 1500 m s^{-1} through seawater. Due to the relatively shallow nature of the sedimentary features, we also assume a velocity of 1500 m s^{-1} for subsurface travel of waves. With this assumption we obtain a minimum estimate for the thickness of sedimentary units. The maximum penetration achieved by Chirp sub-bottom sediment profiles is approximately 30 m. Table 1 summarizes the ^{14}C ages referred to in the text and in Fig. 1. All dates were recalibrated using Calib 7.1 (Stuiver & Reimer 1993) and the MARINE13 calibration curves (Reimer *et al.* 2013). A ΔR value of 105±24 was applied for local effects on the global reservoir correction in the Arctic (Mangerud *et al.* 2006).

Results and interpretation

The bathymetric and subsurface data reveal a complex network of interlinked geomorphological features, which are categorized based on similarities in form, geometry, size and composition. Here we describe and interpret a large, trough-transverse sedimentary ridge (Figs 2, 3) and an assortment of sea-floor grooves (Figs 4, 5), which are split into single grooves and sets of parallel grooves.

Sedimentary wedges and fans: grounding-zone deposits

Observations. – The bathymetric survey reveals a 43-km-long slope break, 60 km east of the continental shelf edge and orientated approximately north–south

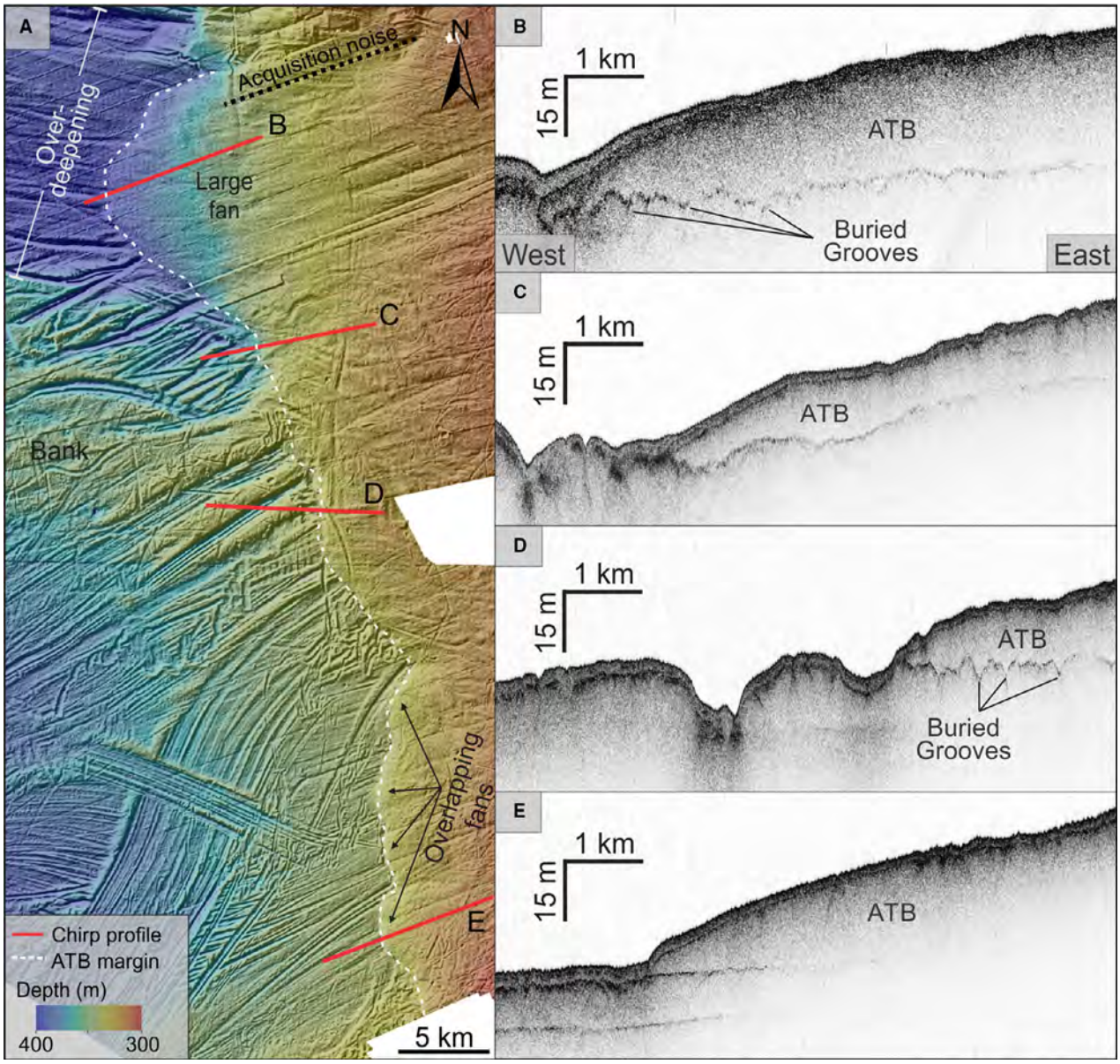

Fig. 2. A. Sea-floor bathymetry at the western edge of an acoustically transparent body (ATB), mapped using Chirp sub-bottom sediment profiles. B–E. Chirp sub-bottom profiles along the ATB.

(Figs 2, 3). Shallow acoustic and 2D seismic profiles across the break in slope reveal a uniform, acoustically transparent sedimentary unit with relatively few low-amplitude seaward-dipping reflections (Figs 2B–E; 3B, C). Sediment packages with similar acoustic properties are referred to as an acoustically transparent sediment body (ATB) (e.g. Elverhøi *et al.* 1983) and are described in the neighbouring Kveithola trough (Rebesco *et al.* 2011; Bjarnadóttir *et al.* 2013) and elsewhere in the Barents Sea (Hogan *et al.* 2010; Andreassen *et al.* 2014; Bjarnadóttir *et al.* 2014). Forty Chirp sub-bottom profiles and two 2D seismic profiles were utilized to map the western margin of the ATB, and the eastern extent (Fig. 2A) is interpolated between the two seismic profiles (Fig. 3B, C), and three Chirp sub-bottom profiles where penetration was sufficient.

The ATB has a convex western termination and thickens towards the east, forming an approximate wedge shape up to 120 m thick in the north and up to 25 m thick in the south (Fig. 3B, C). Based on the available subsurface data, we estimate that it spans a minimum area of 1152 km^2 and extends up to 30 km in the east–west orientation of the trough. In the north, the sea floor west of the ATB is 15 to 20 m deeper than surrounding areas (Fig. 3A), and Pedrosa *et al.* (2011) show that the depression becomes shallower towards the west, terminating at a ridge on the shelf edge. The ATB margin therefore terminates on a retrograde bed in the

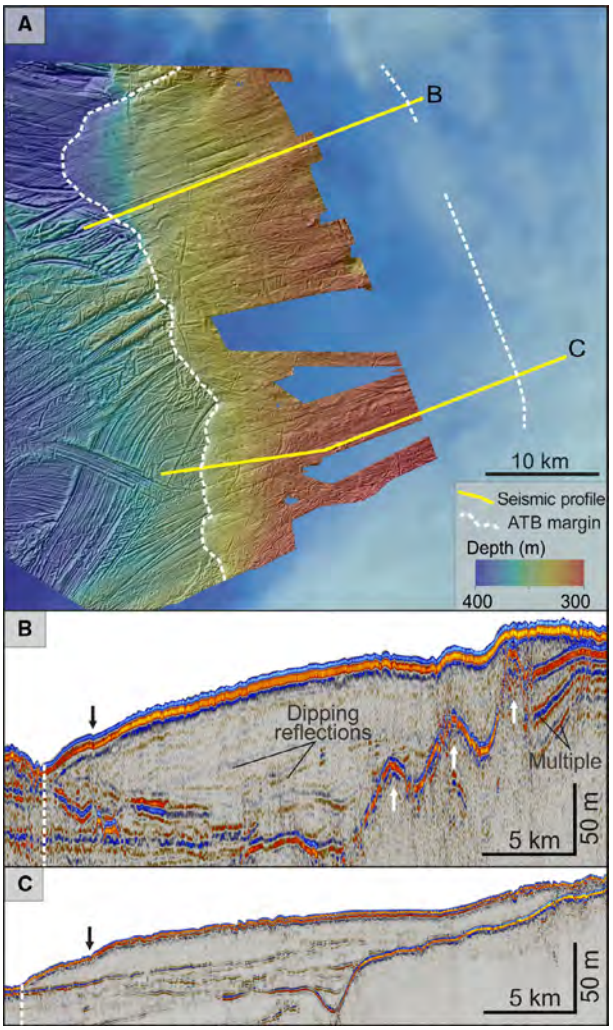

Fig. 3. A. Sea-floor bathymetry across the full extent of the acoustically transparent body (ATB), with eastern extent and thickness mapped using 2D seismic profiles (B) in the north and (C) in the south. Dotted white line shows the extent of the ATB, black arrows point to steps in the long profile, and white arrows point to basal ridges.

north. A buried acoustic reflector is observed in Chirp sub-bottom profiles at the western edge of the ATB (Fig. 2B–E), which varies along its length from being relatively smooth (Fig. 2E), to containing sharp undulations (buried grooves: Fig. 2B, D).

Both the bathymetric and acoustic data sets show clear differences in the form and surface morphology of the ATB along its length, with a large protruding fan in the north and smaller overlapping fans characterizing the southern edge (Fig. 2A). The large fan in the north of the area has a smooth sea-floor surface (Fig. 2B) and is situated in the deepest water depths (up to 400 m) along the ATB margin. Shallow acoustic profiles reveal an undulating reflector beneath the fan, which can be traced for approximately 9 km beneath the ATB (Fig. 2B). On 2D seismic data, a high amplitude reflector marks the base of the ATB in the north (Fig. 3B), and from SW to NE this surface deepens towards the middle, before shallowing steeply towards the eastern margin of the ATB. Below the eastern end of the high amplitude reflector is a repeating pattern of phase reversed reflections that become increasingly steeper with depth, labelled 'multiple' on Fig. 3B. To the east, the basal reflector contains three large ridges 30 to 75 m high (white arrows: Fig. 3B), the highest of which coincides with the approximate eastern extent of the ATB. The western margin of the southern sector of the ATB comprises four coalescing smaller fans (average widths of 3.3 km) spaced approximately 3 km apart that are otherwise similar in planform to the large fan in the north (Fig. 2A). The ATB long profile here contains a small step (Fig. 3C) and the buried reflector is relatively smooth (Figs 2E, 3C).

Interpretation. – The trough-transverse ATB with wedge-shaped cross-section (Figs 2B–E, 3B, C) is consistent with descriptions of grounding-zone deposits (GZD), formed through accumulation of sediments at the grounding zones of marine-terminating ice streams (Powell 1990; Powell & Alley 1997; Ottesen & Dowdeswell 2006; Koch & Isbell 2013). We suggest that the observed ATB is an intermediate feature on a continuum of described grounding-zone features formed depending on the relative abundance of subglacial meltwater, between end-member features 'Morainal Banks' characterized by ice-proximal fans on their ice-distal edge, and GZW, characterized by asymmetric geometry and homogenous, fine-grained sediments (Powell & Alley 1997; Batchelor & Dowdeswell 2015). The GZD described in this study exhibits characteristics of both 'end-member' landforms.

We suggest a build-up of material via line-sourced deposition of subglacial and englacial debris over the grounding-line, accounting for the trough-transverse, asymmetric nature of deposited sediments (Figs 2, 3). Based on the large fan in the north and overlapping fans in the south, we also suggest contributions to sediment accumulation from suspension settling out of meltwater plumes discharged from ice-margin subglacial meltwater outlets. Point-sourced meltwater plumes and sediment gravity flows at the palaeo-ice margin contribute to the build-up of grounding-line proximal fans (e.g. Powell & Molnia 1989; Powell & Domack 2002), and this fanned morphology (Fig. 3A) is similar to GZD described in the neighbouring trough, Kveithola (Rebesco *et al.* 2011; Bjarnadóttir *et al.* 2013). Longer suspended sediment plumes are associated with higher meltwater velocities and channel discharge (Syvitski 1989), and the single-fan morphology of the northern parts of the GZD (Fig. 2A) suggests formation by a singular meltwater conduit and associated meltwater plume. Steps in the long profile (Fig. 3A, B) might reflect periods of meltwater conduit inactivity and associated reductions in sediment deposition, which in conjunction with continued ice-margin

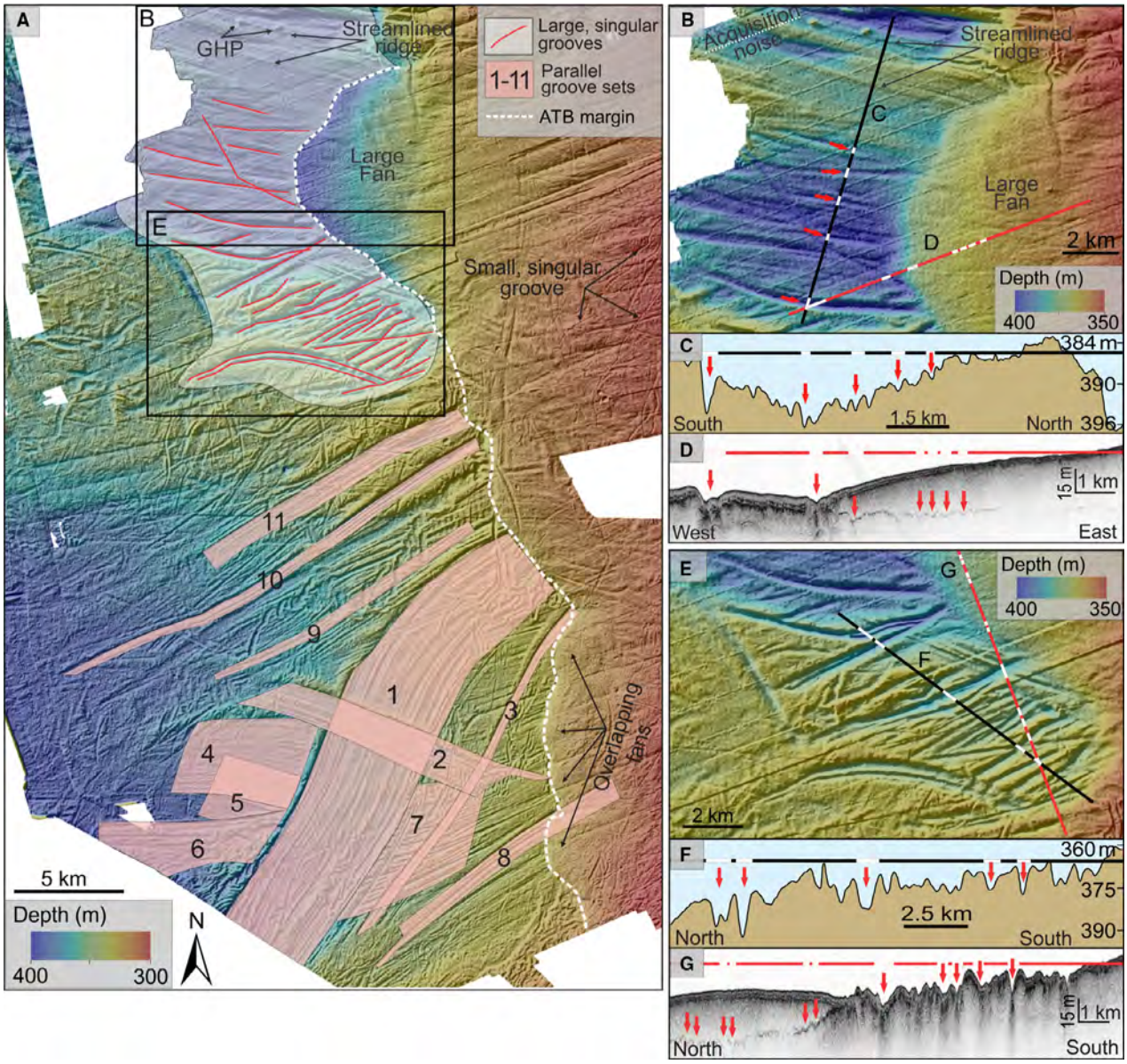

Fig. 4. A. Distribution of sea-floor ridges and grooves, highlighting the locations of deep, single grooves and with numbered sets of parallel grooves. GHP = gas hydrate pingos. B. Singular, east–west orientated grooves to the north of the region, with (C) cross-profile showing water depth and groove dimensions, and (D) subsurface profile indicating buried grooves beneath the large fan. E. Deep singular grooves to the south of the large fan, with (F) cross-profile showing water depth and groove dimensions, and (G) subsurface profiles showing grooves buried by the large fan.

retreat eastwards would result in steps, following conduit reactivation and resumed deposition.

In contrast, the coalescing fans that comprise the southern sector of the ATB are interpreted to have been shaped by sedimentation from multiple or shifting point sources (i.e. subglacial conduits). Basal water conduits are prone to shifting location, and seasonal differences in meltwater input, shifting ice dynamics and changing ice thickness influence glacier hydrology (e.g. Clark & Walder 1994), all factors which are prominent during deglaciation. Iceberg calving may have also played a role in conduit switching on/off or shifting location, by exposing new faces of the ice front and altering ice margin geometry (Syvitski 1989). The fans may be smaller here than in the north due to lower water velocities in the channels and reduced plume length, limiting the capacity to carry suspended sediment far beyond the ice margin.

Curvilinear grooves: single-keeled iceberg ploughmarks

Observations. – Large curvilinear grooves are observed on the sea floor, particularly to the north of the bathymetric survey area (Fig. 4A). East–west trending grooves in the north (Fig. 4B) are no more than 2 m deep

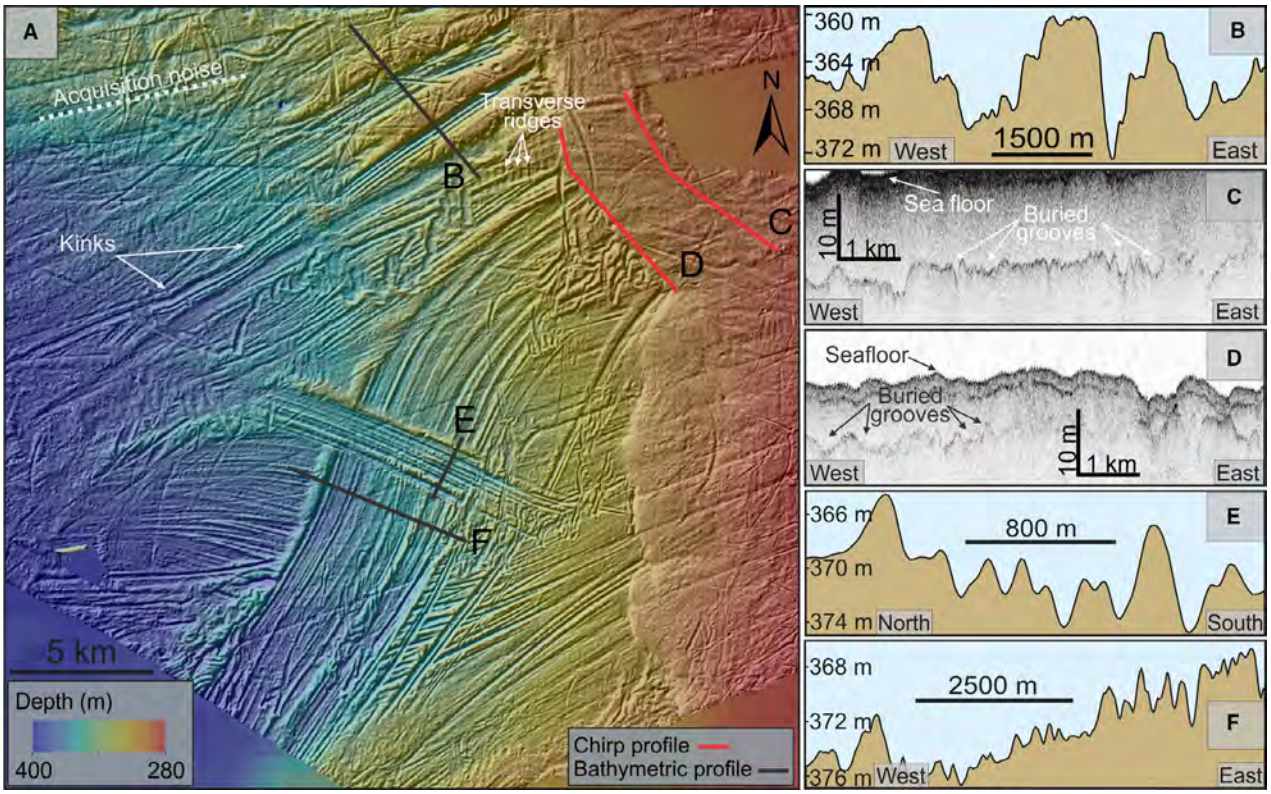

Fig. 5. A. Sea-floor bathymetric map presenting sets of parallel sea-floor grooves. Bathymetric profiles (B, E, F) and CHIRP sub-bottom profiles (C, D) show cross-profiles of groove sets on and beneath the sea floor.

(Fig. 4C) with lengths reaching at least 7.6 km (most extend beyond survey area). Cross-cutting is common, and the majority of grooves are flanked on either side by small berms (Fig. 4B–G). Correlation between grooves observed in bathymetric data and grooves observed in subsurface data (Fig. 4B, D) suggest that the grooves visible on the sea floor extend beneath the GZD. A deeper and wider population of northeast–southwest orientated curvilinear grooves is clustered immediately south of the larger ice-proximal fan (Fig. 4E–G), and most of them terminate where the sea floor shallows to the west (Fig. 4E). The grooves are 1 to 12 m in height from trough to peak and up to 9 km in length (Fig. 4E). Subsurface data show that at least one of the grooves has been partially buried by the GZD (Fig. 4G), indicating that this and potentially other features initiate beneath the deposits.

To the far north of the bathymetric survey area, several linear features are observed with similar orientations to the curvilinear grooves, although resembling streamlined ridges. The ridges are found in the deepest water depths of the available bathymetric data (up to 400 m), in a small area absent of sea-floor grooves. The ridges are several metres high and over 8 km long, extending beyond the survey area (Fig. 4B). Two circular mounds (Fig. 4A) overprint the ridges, which have been previously interpreted as gas-hydrate pingos (Serov *et al.* 2017). Curvilinear grooves with smaller widths and depths than those described above are common throughout the survey area (Fig. 4A), typically <1 m wide and <2 m deep. The

Table 2. Summary of the differences in geomorphological and environmental characteristics between the northern and southern sectors of outer-Storfjordrenna.

	Northern sector	Southern sector
Catchment area (setting)	Svalbard (terrestrial)	Barents Sea (marine)
Bed slope	East-dipping (retrograde slope)	West-dipping (positive slope)
GZD western margin morphology	Large, single sedimentary fan	Small, coalescing sedimentary fans
GZD max. thickness	120 m	25 m
Iceberg calving	Majority deep, single-keeled icebergs	Majority large, multi-keeled icebergs
Topographic pinning	Lateral (Spitsbergen) and basal (bedrock ridges)	Limited lateral (Spitsbergenbanken)
Water depth at ice margin	Deeper (370–400 m)	Shallower (364–370 m)

smaller grooves change direction often and by up to 180 degrees, regularly cross-cutting each other and other geomorphic features, generally with small berms on either side. The small grooves are the only resolvable features that overlie the GZD.

Interpretation. – Based on their curvilinear planform, flanking berms, and frequent cross-cutting, both the shallower and the deeper/wider curvilinear grooves (Fig. 4A–G) are interpreted as iceberg ploughmarks, formed through scouring of the seabed by the keel of large icebergs. Similar features have been observed elsewhere in the Barents Sea (e.g. Andreassen *et al.* 2014), in the Canadian Arctic (e.g. MacLean *et al.* 2010) and Antarctic (e.g. Graham *et al.* 2016) and are interpreted as evidence of iceberg keel scour. The difference in depth between iceberg ploughmarks to the west and to the south of the large fan (Fig. 4A) can be explained by the 15–20 m difference in water depth (Fig. 3A), limiting iceberg keel scouring in the deeper waters. Furthermore, relatively high sediment infilling of sea-floor features is expected in the north, associated with the high rate of sediment delivery beyond the ice margin from the inferred large subglacial meltwater outlet and associated plume.

Based on their high length to width ratio, the streamlined ridges to the far north of the survey area (Fig. 4B) are interpreted as mega-scale glacial lineations (MSGL), formed subglacially at an earlier stage to other features discussed here, when the ice stream was grounded at or close to the continental shelf break. MSGL occurrence in the deepest water along the former margin suggests that lineations must be preserved because they are located below the depth of iceberg grounding, limiting sea-floor scouring and landform overprinting. Smaller grooves with highly variable orientations are interpreted to have been formed through iceberg keel scour from icebergs of a smaller scale to that previously described. Such features are ubiquitous at the marine margins of both palaeo- and present-day ice streams and outlet glaciers (e.g. Lien *et al.* 1989; Dowdeswell & Ottesen 2013; Livingstone *et al.* 2013; Esteves *et al.* 2017), and their highly variable orientations and sudden changes in direction are attributed to changes in ocean currents and surface winds (Smith & Banke 1983). As the only grooved feature present on top of the GZD, smaller grooves indicate continued calving of single-keeled icebergs subsequent to the deposition of grounding-zone sediments.

Sets of parallel curvilinear grooves: multi-keeled iceberg ploughmarks

Observations. – Sets of parallel grooves are observed on the sea floor mainly in the south of the bathymetric survey area (Figs 4A, 5), and are also traced beneath the southern parts of the GZD on subsurface data (Fig. 5C, D). The sets have a wide range of widths, from 300 m to 4.6 km, and the number of grooves per set is variable and not necessarily correlated to width. The GZD covers the full eastern extent and origin of most groove sets, and some extend downstream beyond the survey area (Fig. 4A). Lengths range from several km to a minimum of 22.3 km, and the number of grooves in each set generally diminishes with increasing water depth. Kinks within otherwise straight sets of grooves occur in the thinner sets (Fig. 5A) and some have large berms on either one or both edges (Fig. 5A).

The largest of the groove sets (Set 1; Fig. 4A) has a consistent width of 4.6 km and is at least 21 km long, spanning water depths between 350 to 380 m (Fig. 5A, F), although the upstream extent is covered by the GZD, and the downstream extent lies beyond the bathymetric survey area. Subsurface data indicate that the grooves extend beneath the GZD a minimum of 3.6 km (Fig. 5C, D). Ridges and grooves vary in height throughout Set 1, between 0.5 and 5 m from trough to peak (Fig. 5F). The northwestern flank is bordered by a berm up to 5 m high and 600 m wide (Fig. 5A). Cutting across the largest groove set at 90° is a narrower set (Set 2; Fig. 4A) up to 2 km in width (Fig. 5E), with most grooves initiating away from the GZD edge. Set 2 has a berm only on its northern flank (Fig. 5A), and originates with two parallel grooves 1.8 km in length extending from beneath the GZD, before the initiation of eight more grooves extending west-northwest for 11 km. Groove sets 1 and 2 overprint an array of older sets of predominantly east–west trending parallel grooves (Fig. 4A). Additionally, one set of grooves contains regularly spaced transverse ridges 1 to 2 m high, with consistent spacing of approximately 500 m (Fig. 5A).

Interpretation. – Sets of parallel, curvilinear grooves are interpreted to have formed through seabed scouring by multi-keeled icebergs, based on their curvilinearity, kinks in their long profile, flanking berms, and diminishing number of grooves per set with increasing depth. Large, tabular icebergs calving off the ice-stream terminus with extruding keels at their base are interpreted to have scoured the sea floor as they advanced westwards. Burial of ploughmarks by material comprising the GZD indicates that sea-floor scouring occurred before the deposition of the GZD. The close spacing and organization of grooves into discrete sets indicate that they have been ploughed by large multi-keeled icebergs rather than by many smaller, single-keeled icebergs trapped in multi-year sea ice. Such features have been described in Antarctica (Lien *et al.* 1989; Dowdeswell & Bamber 2007; Wise *et al.* 2017), the Central Barents Sea (Andreassen *et al.* 2014; Bjarnadóttir *et al.* 2014), the northern Svalbard margin (Hogan *et al.* 2010) and the Canadian Arctic (MacLean *et al.* 2010). Transverse ridges spanning several grooves (Fig. 5A) are interpreted as corrugation ridges, formed by diurnal tidal forcing on grounded icebergs (Jakobsson *et al.* 2011, 2012). Corru-

gation ridges with comparable widths, heights and spacings are described in Pine Island Bay, West Antarctica (Jakobsson *et al.* 2011; Graham *et al.* 2013), and on the northern Svalbard shelf (Bjarnadóttir *et al.* 2014; Dowdeswell & Hogan 2014).

Discussion

The grounding-line landform assemblages described and interpreted in outer-Storfjordrenna demonstrate clear differences in morphology between the northern and southern sectors (summarized in Table 2). The following sections discuss the significance of the documented variations in the context of ice-stream characteristics and margin retreat, grounding-zone deposition and subglacial hydrology, and iceberg calving and seabed scouring.

Ice-stream characteristics and margin retreat

The Storfjordrenna Ice Stream had a large and varied catchment, with the northern parts of the trough fed by ice draining from terrestrial Svalbard through Storfjorden, and the southern parts fed by ice draining the interior of the marine-based Barents Sea Ice Sheet and Spitsbergenbanken (Fig. 1). Ice is therefore sourced from three different ice-sheet settings: from areas at relatively high bed altitude and stable ice sources over Svalbard; from the interior of the ice sheet with low-lying bed and fluctuating ice domes; and from the relatively shallow and topographically featureless Spitsbergenbanken closer to the ice-sheet periphery. Contrasting ice sources governing ice thicknesses and temperature regimes could have regulated crevasse spacing and distributions across the former ice margin after the ice converged, producing the observed spatial clustering of distinct iceberg scouring. Previous studies propose that the Storfjordrenna Ice Stream was comprised of three distinct ice-stream lobes while grounded at the shelf break (Pedrosa *et al.* 2011; Lucchi *et al.* 2013; Llopart *et al.* 2015), and our findings show that the ice stream also maintained distinct lateral variations, at least in terms of iceberg production, during the initial stages of deglaciation. We also interpret the differences in GZD morphology and iceberg scouring between the northern and southern sectors of outer-Storfjordrenna to reflect variations in ice stream characteristics across the trough.

Based on the onset of hemipelagic sediment and ice-rafted debris (IRD) concentration peaks in sediment cores from the TMF and outer shelf, the initiation of deglaciation in Storfjordrenna is estimated at around 20 to 19 cal. ka BP through increased iceberg calving (Rasmussen *et al.* 2007; Jessen *et al.* 2010). Break-up of the ice margin via large calving events is supported here by overlapping sets of ploughmarks created by large, tabular icebergs. Observations of coarse-massive-IRD subfacies during deglaciation in cores from the Storfjordrenna TMF (Lucchi *et al.* 2013) suggest intermittent periods of intense calving activity. This, together with the evidence presented herein for high magnitude iceberg calving events and subsequent grounding-line stabilization indicates that retreat of the Storfjordrenna Ice Stream was episodic in nature (cf. Dowdeswell *et al.* 2008), at least from the continental shelf edge. Episodic ice retreat is also documented by a series of GZW in upstream Storfjorden, deposited during the later stages of deglaciation between 15 and 10 cal. ka BP (Nielsen & Rasmussen 2018). Minimum deglacial dates in Storfjordrenna to the west and east of the GZD imply 200 km ice-margin retreat over approximately 7900 years, indicating a relatively slow averaged margin retreat rate of 0.025 km a^{-1} (Fig. 1, Table 1; Rasmussen *et al.* 2007; Rasmussen & Thomsen 2014; Patton *et al.* 2015). Time scales of GZD sedimentation are uncertain, but based on similar large grounding-zone sediment accumulations in other regions, it is reasonable to assume that the ice margin in Storfjordrenna remained stable here for at least several decades to centuries (Batchelor & Dowdeswell 2015).

Retreating grounding-lines are stabilized by pinning points, such as increasingly narrow trough/fjord mouths and topographic highs under basal ice (Thomas 1979; Benn *et al.* 2007a; Jamieson *et al.* 2012). We propose that the three ridges 30 to 75 m high observed in seismic data at the eastern edge of the GZD (Fig. 3B) provided basal pinning points stabilizing the retreating Storfjordrenna Ice Stream margin. Furthermore, the protruding southern tip of Spitsbergen provides a lateral pinning point for the ice stream while it was grounded in outer-Storfjordrenna. The relatively non-scoured upper surface of the GZD suggests that either calving was minimal subsequent to margin stabilization and GZD deposition, or that the ice margin was floating, with ice already in buoyant equilibrium with the ocean water prior to calving, resulting in no significant drop in height or seafloor scouring. A floating ice shelf would also extend the calving margin well away from the grounding-line, preserving the surface of the GZD from iceberg scouring. It is difficult to determine whether the ice margin had a substantial floating ice shelf, although GZW build-ups at other reconstructed ice margins are associated with a sub-shelf cavity beneath floating ice (Batchelor & Dowdeswell 2015). We tentatively suggest that the Storfjordrenna Ice Stream margin was floating while the grounding-line was stabilized in outer-Storfjordrenna, based on the non-scoured surface of the GZD and the asymmetric shape of deposited sediments, which suggest deposition within a sub-shelf cavity.

Retrograde bed slopes underlaid the northern sectors of the ice stream over much of the former bed, enhanced by the overdeepened sector west of the GZD (Fig. 1B). In contrast, the bed of the southern lobe has a gentle upward-sloping inland gradient. Cores from the outer shelf indicate that sediment accumulations since the

deposition of glacial till are an order of magnitude lower than the 40-m elevation difference between the outer and outer shelf (Rasmussen *et al.* 2007), ruling out a post-ice retreat origin for the retrograde bed slope. Ice margins become more unstable with increasing water depth, and margin retreat into deeper waters results in positive feedback, whereby retreat is perpetuated until a seaward-dipping bed slope or pinning point is encountered (Schoof 2007; Jamieson *et al.* 2012). We suggest a topographic influence on earlier ice-stream retreat in the north of the area, in addition to the proximal ice sources suggested by Pedrosa *et al.* (2011), where retrograde bed slopes facilitated runaway margin retreat through outer-Storfjordrenna. A relatively deeper ice-bed in the northern part of the outer trough (Fig. 1B) could result from a more dynamically active and erosive ice stream here. Increased sediment fluxes and earlier ice-margin stabilization in outer-Storfjordrenna for the northern sectors of the ice stream also fits well with our observations, as the northern parts of the GZD are thicker than those farther south (Fig. 3B, C).

The occurrence of iceberg ploughmarks declines in water depths below 380 m (Fig. 4A), indicating a depth limit to keel scouring, and therefore revealing an upper limit to potential iceberg thicknesses. Assuming a eustatic sea level adjustment of 120 m lower than present day and isostatic depression of approximately 80 m following the LGM (Peltier & Fairbanks 2006; Auriac *et al.* 2016; Patton *et al.* 2017), we estimate that icebergs calved from the ice-stream margin when it was grounded in outer-Storfjordrenna had keels approximately 340 m deep. Given that icebergs are generally 90% submerged below the sea surface, a rough estimate of iceberg and ice-margin thickness is 380 m.

The geomorphology discussed herein is a record of two main phases of ice-stream activity: ice-margin retreat from the shelf break, and grounding-zone stabilization in outer-Storfjordrenna. Ice-margin retreat from the continental shelf break is documented by large, multi-keeled iceberg ploughmarks created by tabular icebergs calved as the ice margin broke up during early deglaciation. During this phase, we suggest that the bathymetric differences between the northern and southern sectors of the former ice-stream bed influenced the asynchronous retreat. Subsequent to this initial retreat, the grounding-line and ice margin stabilized in outer-Storfjordrenna, with sediments continuously being delivered and deposited at the grounding zone, building up the GZD. During this phase, we suggest that lateral and bed pinning from southern Spitsbergen and underlying bedrock ridges were important factors determining the location of margin stabilization.

Grounding-zone deposition and subglacial hydrology

The large accumulation of grounding-zone sediments described here potentially evidences the first major standstill in grounding-line retreat during the deglaciation of the Storfjordrenna Ice Stream. The build-up of the majority of sediments via progradational, line-source deposition of subglacial and englacial debris over the grounding-line leads to the overall wedge-shaped cross-section of deposited material (Figs 2B–E, 3B, C). However, the fanned morphology at the northern and southern parts of the GZD (Fig. 2A) also indicates point-sourced sedimentation out of ice-marginal meltwater conduits and associated plumes. In Kveithola, the neighbouring trough to Storfjordrenna (Fig. 1A), a meltwater-influenced grounding-zone landform is described and interpreted similarly (Bjarnadóttir *et al.* 2013), indicating that comparable grounding-zone processes were operating here to those described in Storfjordrenna. Significant subglacial meltwater activity at the ice margin is further supported by sedimentary data from the continental slope, where gullies and laminated sediment sequences on the Storfjordrenna TMF are attributed to rapid sediment deposition from subglacial meltwater plumes (Lucchi *et al.* 2012).

Subglacial drainage routing is primarily controlled by the geometry and thickness of overlying ice, which directs subglacial water from areas of high pressure under thicker ice to areas of lower pressure under thinner ice (Shreve 1972). The occurrence of ice-proximal fans in the north and south of Storfjordrenna and lack of evidence for meltwater-related deposition in between (Fig. 2A) may therefore reflect thicker ice flowing in the centre of the trough. Modelled subglacial drainage routing predicts margin outlets for large drainage basins in the northern sector of Storfjordrenna consistently throughout deglaciation (cf. Shackleton *et al.* 2018: fig. 8), therefore supporting the focused drainage routing and large ice-marginal meltwater outlet and plume that we propose in the north. This also explains the difference in thickness of glacigenic diamicton in cores from the TMF, which varies from over 45 m in the northern sectors to 20 m in the southern sectors, despite longer ice-margin residence time at the shelf break in the south during the LGM (Lucchi *et al.* 2013). Furthermore, several drainage outlets are predicted in the south by hydraulic potential modelling (Shackleton *et al.* 2018), but only when the ice margin was stabilized in outer-Storfjordrenna. Predicted outlets in the south also drained much smaller catchments, thereby supporting our reconstructions of lower-velocity meltwater plumes with fluctuating levels of activity. Stable drainage outlets in the north may be a consequence of a catchment comprised of more stable ice over Svalbard, in contrast to the shifting catchments feeding the southern sector, more susceptible to fluctuations in ice flux, geometry and thickness especially as the Barents Sea Ice Sheet deglaciated.

At the southern sector of the former ice margin, average spacings of 3 km between the four overlapping fans (Fig. 3A) suggest that a singular, shifting meltwater outlet or several outlets with plumes of 3 km spacing may

have been active at the former ice margin. Comparably, marginal meltwater outlets and suspended sediment plumes with the same average spacings of 3 km are observed at the margin of the Austfonna ice cap, northeast Svalbard, and have remained stable for several decades (Dowdeswell *et al.* 2015). Subglacial outflow across the former margin and the formation of meltwater plumes indicate that the pressure of subglacial water must have been substantial, with potential implications for the stability of the grounding-line. Lower effective pressures as a result of high-pressure basal water can facilitate increased ice velocities (Alley 1989), leading to increased flux of ice over the grounding-line, and potentially increasing mass loss at the northern and southern sectors of the former ice margin in Storfjordrenna. Additionally, large meltwater outlets at the margin can lead to localized retreat of the ice front (Slater *et al.* 2015), forming embayments with laterally protruding ice either side. This may have left more of the margin open for calving and ocean driven melting, especially in the north where we infer a stable, high-discharge meltwater conduit.

Iceberg calving and seabed scouring

Extensive iceberg keel scouring in outer-Storfjordrenna (Fig. 4A) documents significant calving activity during the initial stages of deglaciation, and furthermore records local variations in calving characteristics between the northern (single-keeled icebergs) and southern (multi-keeled icebergs) sectors of the ice stream. Multi-keeled iceberg ploughmarks tracing beneath the GZD (Fig. 5A, C, D) imply formation during initial ice-margin break-up and retreat from the continental shelf edge, before the grounding-line stabilized in outer-Storfjordrenna. However, the relative timing of the calving of deep, single-keeled icebergs in the north is uncertain and may not have occurred contemporaneously. An increased frequency of iceberg calving is associated with increasing water depth, due to greater ice-marginal buoyancy (Benn *et al.* 2007b), and variations in calving characteristics between the north and south might therefore be a consequence of the difference in water depth at the former ice margin. This could promote a higher frequency of calving events, producing large, single-keeled icebergs in the north where water was deeper, and a lower frequency of multi-keeled, tabular icebergs calved in the south.

Iceberg geometry is primarily determined by crevasses within glacial ice, which can be advected passively to the terminus (Motyka *et al.* 2011) or develop *in-situ* due to stresses exerted at the margin (Benn *et al.* 2007a). Tabular icebergs are associated with crevasse/rift opening by glaciologically derived stresses rather than oceanic or atmospherically derived forcing (Joughin & Macayeal 2005). Hence, the calving of large tabular icebergs in the southern sector of Storfjordrenna might be linked to glaciologically controlled crevasse formation and crevasse spacings set upstream of the grounding zone. Furthermore, several hypothesized ice-stream lobes converged in central Storfjordrenna to flow towards the continental shelf edge (Fig. 1), and longitudinal stress gradients inherent in these separate ice-stream lobes before they converged would become even greater once converged (Benn *et al.* 2007a), leading to large numbers of deep crevasses advected to the margin. Lateral pinning from the southern tip of Svalbard and Spitsbergenbanken may also have provided resistance through lateral drag, which would generate strong velocity gradients, leading to higher strain rates and consequently more crevasses and calving events. The clustering of large, single-keeled iceberg ploughmarks in the north and multi-keeled, tabular icebergs in the south (Fig. 4A) might also therefore reflect continued production of distinct strain-induced crevasses as the ice-stream lobes interacted upstream.

Subglacial meltwater drainage at the margin may also influence iceberg calving characteristics, associated with undercutting and selective erosion of the ice margin from marginal meltwater outlets (Syvitski 1989; Slater *et al.* 2015). Development of ice caves and undercut ice protrusions in the Storfjordrenna Ice Stream would have led to increased iceberg calving and embayments forming, potentially leaving a protruding ice face in the centre of the trough. Furthermore, plume-driven submarine melting can undercut the submerged portion of the calving front, which may lead to submarine iceberg calving (Rignot *et al.* 2010) and/or more rapid rates of calving (Motyka *et al.* 2003). Channelized meltwater and freshwater plumes can influence local ocean circulation, leading to convective cells upwelling cold, buoyant glacial meltwater at the surface, and drawing in warmer seawater to the margin at depth, leading to increased melting near the grounding-line (Jenkins 2011; Motyka *et al.* 2011; Chauché *et al.* 2014; Kimura *et al.* 2014). These convective cells may have influenced the movement of icebergs and resulting keel scour orientation, which is generally the same direction as inferred palaeo-ice stream flow (Fig. 4A).

Sea ice and/or ice melange acts as a buffer to iceberg calving, providing longitudinal backstress, whilst also preventing existing icebergs from floating away from the calving margin (Amundson *et al.* 2010). An ice melange may also strengthen sufficiently to inhibit the overturning of large, unstable icebergs, providing a mechanism by which icebergs may resist overturning. The influence of ice melange on calving and subsequent seabed scour is well evidenced at two localities in the neighbouring Bjørnøyrenna Palaeo-Ice Stream bed (Andreassen *et al.* 2014; Bjarnadóttir *et al.* 2014). Icebergs stuck fast within an ice melange or multi-year sea ice are also plausible in Storfjordrenna, given reconstructed winter surface water temperatures 1 °C above freezing for the southeastern Svalbard margin between 20 and 15 ka BP (Rasmussen

et al. 2007). Compatibly, Lucchi *et al.* (2013) propose that multi-year sea ice could explain occasional reductions in IRD on the Storfjordrenna TMF during deglaciation. We suggest that break-up of an ice melange containing stuck-fast tabular icebergs is a potential cause of the sudden initiation of multi-keeled iceberg ploughmark set 2 (Fig. 4A), and that melange-led drift of trapped icebergs might further explain the consistent west-southwest direction of keel scour in this region.

Conclusions

We present new geophysical data from a large glacial trough, Storfjordrenna, which contain geomorphological evidence for stabilization of the retreating Storfjordrenna Ice Stream margin as it deglaciated from its maximum extent at the continental shelf break. Seabed and subsurface investigations of this former grounding zone reveal a trough-transverse wedge of sediments, with protruding sedimentary fans, interpreted as a GZD comprised of both line-sourced, glacigenic sediments and point-sourced glacifluvial sediments deposited out of marginal meltwater plumes. Curvilinear grooves on the sea floor indicate concentrated scouring by the keels of large icebergs. The geomorphology presented here contributes to an increased understanding of Storfjordrenna Ice Stream glacial history, documenting two main phases of ice-stream activity: ice-margin retreat from the continental shelf break, and a subsequent period of stabilization of the retreating grounding-line. Partial burial of iceberg ploughmarks indicates that the scouring of large sets of parallel grooves occurred during initial retreat of the ice margin through outer-Storfjordrenna, through ice-margin break-up into large, tabular icebergs. Earlier ice margin retreat in the north was probably facilitated by retrograde bed slopes on the outer shelf and proximal ice sources over Spitsbergen, with margin stabilization promoted by lateral and bed pinning points at the southern tip of Spitsbergen.

Local environmental differences along the length of the former ice margin had strong impacts on ice-margin stability and grounding-zone deposition, and may be relevant for reconstructions of recently deglaciated ice margins and predicting changes to present-day ice margins. The fanned surface morphology of the GZD suggests that subglacial meltwater outlets and plumes contributed to the build-up of grounding-zone sediments here, indicating that meltwater conduits were active during retreat. Subglacial drainage at the ice margin may have influenced the stability of the grounding-line through regulation of basal hydraulic pressure, and influenced iceberg calving by undercutting and shaping the ice margin. Spatial clustering of single-keeled iceberg ploughmarks in the north and multi-keeled iceberg ploughmarks at the southern sector of the former ice margin suggest that iceberg calving at the northern sector was characterized by deep-drafted, single-keeled icebergs, and the southern sectors by large, tabular icebergs. Greater water depths at the northern sector of the ice margin probably contributed to differences in the character of calved icebergs, the scouring of the sea floor by iceberg keels, and the preservation of older landforms.

Acknowledgements. – This research is part of the Centre for Arctic Gas Hydrate, Environment and Climate and was supported by the Research Council of Norway through its Centres of Excellence funding scheme, grant no. 223259. We thank R. Minzoni and B.J. Todd for thorough and constructive reviews, which significantly improved the manuscript, and the captain and crew of the R/V 'Helmer Hanssen' and engineers Steinar Iversen and Anoop Nair for their role in the collection and processing of geophysical data.

Author contributions. – CS, KA and MW were responsible for the data collection and processing. CS undertook the analysis and wrote and edited the manuscript with scientific input and editing from MW, KA, RL and LB. All authors were involved in interpreting the bathymetric data and discussing the scientific content.

References

Alley, R. B. 1989: Water-pressure coupling of sliding and bed deformation: 1. Water system. *Journal of Glaciology 35*, 108–118.

Amundson, J. M., Fahnestock, M., Truffer, M., Brown, J., Lüthi, M. P. & Motyka, R. J. 2010: Ice melange dynamics and implications for terminus stability, Jakobshavn Isbræ, Greenland. *Journal of Geophysical Research: Earth Surface 115*, F01005, https://doi.org/10.1029/2009JF001405.

Andreassen, K., Laberg, J. S. & Vorren, T. O. 2008: Seafloor geomorphology of the SW Barents Sea and its glaci-dynamic implications. *Geomorphology 97*, 157–177.

Andreassen, K., Winsborrow, M., Bjarnadóttir, L. R. & Rüther, D. C. 2014: Ice stream retreat dynamics inferred from an assemblage of landforms in the northern Barents Sea. *Quaternary Science Reviews 92*, 246–257.

Auriac, A., Whitehouse, P. L., Bentley, M. J., Patton, H., Lloyd, J. M. & Hubbard, A. 2016: Glacial isostatic adjustment associated with the Barents Sea ice sheet: a modelling inter-comparison. *Quaternary Science Reviews 147*, 122–135.

Bassis, J. N. & Jacobs, S. 2013: Diverse calving patterns linked to glacier geometry. *Nature Geoscience 6*, 833–836.

Batchelor, C. L. & Dowdeswell, J. A. 2014: The physiography of High Arctic cross-shelf troughs. *Quaternary Science Reviews 92*, 68–96.

Batchelor, C. L. & Dowdeswell, J. A. 2015: Ice-sheet grounding-zone wedges (GZWs) on high-latitude continental margins. *Marine Geology 363*, 65–92.

Benn, D. I., Hulton, N. R. J. & Mottram, R. H. 2007a: "Calving laws", "sliding laws" and the stability of tidewater glaciers. *Annals of Glaciology 46*, 123–130.

Benn, D. I., Warren, C. R. & Mottram, R. H. 2007b: Calving processes and the dynamics of calving glaciers. *Earth-Science Reviews 82*, 143–179.

Bjarnadóttir, L. R., Rüther, D. C., Winsborrow, M. C. M. & Andreassen, K. 2013: Grounding-line dynamics during the last deglaciation of Kveithola, W Barents Sea, as revealed by seabed geomorphology and shallow seismic stratigraphy. *Boreas 42*, 84–107.

Bjarnadóttir, L. R., Winsborrow, M. C. M. & Andreassen, K. 2014: Deglaciation of the central Barents Sea. *Quaternary Science Reviews 92*, 208–226.

Chauché, N., Hubbard, A., Gascard, J.-C., Box, J. E., Bates, R., Koppes, M., Sole, A., Christoffersen, P. & Patton, H. 2014: Ice–ocean interaction and calving front morphology at two west Greenland tidewater outlet glaciers. *The Cryosphere 8*, 1457–1468.

Clark, P. U. & Walder, J. S. 1994: Subglacial drainage, eskers, and deforming beds beneath the Laurentide and Eurasian ice sheets. *Geological Society of America Bulletin 106*, 304–314.

Dowdeswell, J. A. & Bamber, J. L. 2007: Keel depths of modern Antarctic icebergs and implications for sea-floor scouring in the geological record. *Marine Geology 243*, 120–131.

Dowdeswell, J. A. & Hogan, K. A. 2014: Huge iceberg ploughmarks and associated corrugation ridges on the northern Svalbard shelf. *In* Dowdeswell, J. A., Canals, M., Jakobsson, M., Todd, B. J., Dowdeswell, E. K. & Hogan, K. A. (eds.): *Atlas of Submarine Glacial Landforms: Modern, Quaternary and Ancient*, 269–270. *Geological Society of London, Memoirs 46*.

Dowdeswell, J. A. & Ottesen, D. 2013: Buried iceberg ploughmarks in the early Quaternary sediments of the central North Sea: a two-million year record of glacial influence from 3D seismic data. *Marine Geology 344*, 1–9.

Dowdeswell, J. A., Hogan, K. A., Arnold, N. S., Mugford, R. I., Wells, M., Hirst, J. P. P. & Decalf, C. 2015: Sediment-rich meltwater plumes and ice-proximal fans at the margins of modern and ancient tidewater glaciers: observations and modelling. *Sedimentology 62*, 1665–1692.

Dowdeswell, J. A., Hogan, K. A., Evans, J., Noormets, R., Ó Cofaigh, C. & Ottesen, D. 2010: Past ice-sheet flow east of Svalbard inferred from streamlined subglacial landforms. *Geology 38*, 163–166.

Dowdeswell, J. A., Ottesen, D., Evans, D., Ó Cofaigh, C. & Andersen, J. B. 2008: Submarine glacial landforms and rates of ice-stream collapse. *Geology 36*, 819–822.

Dowdeswell, J. A., Villinger, H., Whittington, R. J. & Marienfeld, P. 1993: Iceberg scouring in Scoresby Sund and on the East Greenland continental shelf. *Marine Geology 111*, 37–53.

Elverhøi, A., Lønne, Ø. & Seland, R. 1983: Glaciomarine sedimentation in a modern fjord environment, Spitsbergen. *Polar Research 1*, 127–150.

Esteves, M., Bjarnadóttir, L. R., Winsborrow, M. C. M., Shackleton, C. S. & Andreassen, K. 2017: Retreat patterns and dynamics of the Sentralbankrenna glacial system, Central Barents Sea. *Quaternary Science Reviews 169*, 131–147.

Graham, A. G. C., Dutrieux, P., Vaughan, D. G., Nitsche, F. O., Gyllencreutz, R., Greenwood, S. L., Larter, R. D. & Jenkins, A. 2013: Seabed corrugations beneath an Antarctic ice shelf revealed by autonomous underwater vehicle survey: origin and implications for the history of Pine Island Glacier. *Journal of Geophysical Research: Earth Surface 118*, 1356–1366.

Graham, A. G. C., Jakobsson, M., Nitsche, F. O., Larter, R. D., Anderson, J. B., Hillenbrand, C.-D., Gohl, K., Klages, J. P., Smith, J. A. & Jenkins, A. 2016: Submarine glacial-landform distribution across the West Antarctic margin, from grounding line to slope: the Pine Island-Thwaites ice-stream system. *Geological Society of London, Memoirs 46*, 493–500.

Hogan, K. A., Dowdeswell, J. A., Noormets, R., Evans, J. & Ó Cofaigh, C. 2010: Evidence for full-glacial flow and retreat of the Late Weichselian Ice Sheet from the waters around Kong Karls Land, eastern Svalbard. *Quaternary Science Reviews 29*, 3563–3582.

Horgan, H. J., Christianson, K., Jacobel, R. W., Anandakrishnan, S. & Alley, R. B. 2013: Sediment deposition at the modern grounding zone of Whillans Ice Stream, West Antarctica. *Geophysical Research Letters 40*, 3934–3939.

Howat, I. M., Box, J. E., Ahn, Y., Herrington, A. & McFadden, E. M. 2010: Seaonal variability in the dynamics of marine-terminating outlet glaciers in Greenland. *Journal of Glaciology 56*, 601–613.

Howat, I. M., Joughin, I. & Scambos, T. A. 2007: Rapid changes in ice discharge from Greenland outlet glaciers. *Science 315*, 1559–1561.

Hughes, A. L. C., Gyllencreutz, R., Lohne, Ø. S., Mangerud, J. & Svendsen, J. I. 2015: The last Eurasian ice sheets - a chronological database and time-slice reconstruction, DATED-1. *Boreas 45*, 1–45.

Ingólfsson, Ó. & Landvik, J. Y. 2013: The Svalbard-Barents Sea ice-sheet-Historical, current and future perspectives. *Quaternary Science Reviews 64*, 33–60.

Jakobsson, M., Anderson, J. B., Nitsche, F. O., Dowdeswell, J. A., Gyllencreutz, R., Kirchner, N., Mohammad, R., O'Regan, M., Alley, R. B., Anandakrishnan, S., Eriksson, B., Kirshner, A., Fernandez, R., Stolldorf, T., Minzoni, R. & Majewski, W. 2011: Geological record of ice shelf break-up and grounding line retreat, Pine Island Bay, West Antarctica. *Geology 39*, 691–694.

Jakobsson, M., Anderson, J. B., Nitsche, F. O., Gyllencreutz, R., Kirshner, A. E., Kirchner, N., O'Regan, M., Mohammad, R. & Eriksson, B. 2012: Ice sheet retreat dynamics inferred from glacial morphology of the central Pine Island Bay Trough, West Antarctica. *Quaternary Science Reviews 38*, 1–10.

Jakobsson, M., Macnab, R., Mayer, L., Anderson, R., Edwards, M., Hatzky, J., Schenke, H. W. & Johnson, P. 2008: An improved bathymetric portrayal of the Arctic Ocean: implications for ocean modeling and geological, geophysical and oceanographic analyses. *Geophysical Research Letters 35*, L07602, https://doi.org/10.1029/2008gl033520.

Jamieson, S. S. R., Vieli, A., Livingstone, S. J., Ó Cofaigh, C., Stokes, C., Hillenbrand, C.-D. & Dowdeswell, J. A. 2012: Ice-stream stability on a reverse bed slope. *Nature Geoscience 5*, 799–802.

Jenkins, A. 2011: Convection-driven melting near the grounding lines of ice shelves and tidewater glaciers. *Journal of Physical Oceanography 41*, 2279–2294.

Jessen, S. P., Rasmussen, T. L., Nielsen, T. & Solheim, A. 2010: A new Late Weichselian and Holocene marine chronology for the western Svalbard slope 30,000-0 cal years BP. *Quaternary Science Reviews 29*, 1301–1312.

Joughin, I. & Macayeal, D. R. 2005: Calving of large tabular icebergs from ice shelf rift systems. *Geophysical Research Letters 32*, L02501, https://doi.org/10.1029/2004GL020978

Katz, R. F. & Worster, M. G. 2010: Stability of ice-sheet grounding lines. *Proceedings of the Royal Society A: Mathematical, Physical and Engineering Sciences 466*, 1597–1620.

Kimura, S., Holland, P. R., Jenkins, A. & Piggott, M. 2014: The effect of meltwater plumes on the melting of a vertical glacier face. *Journal of Physical Oceanography 44*, 3099–3117.

Koch, Z. J. & Isbell, J. L. 2013: Processes and products of grounding-line fans from the Permian Pagoda Formation, Antarctica: insight into glacigenic conditions in polar Gondwana. *Gondwana Research 24*, 161–172.

Laberg, J. S. & Vorren, T. O. 1996: The glacier-fed fan at the mouth of Storfjorden trough, western Barents Sea: a comparative study. *Geographische Rundschau 85*, 338–349.

Łącka, M., Zajączkowski, M., Forwick, M. & Szczuciński, W. 2015: Late Weichselian and Holocene palaeoceanography of Storfjordrenna, southern Svalbard. *Climate of the Past 11*, 587–603.

Landvik, J. H., Bolstad, M., Lycke, A. K., Mangerud, J. & Sejrup, H. P. 1992: Weichselian stratigraphy and palaeoenvironments at Bellsund, western Svalbard. *Boreas 21*, 335–358.

Landvik, J. Y., Bondevik, S., Elverhøi, A., Fjeldskaar, W., Mangerud, J., Salvigsen, O., Siegert, M. J., Svendsen, J.-I. & Vorren, T. O. 1998: The last glacial maximum of Svalbard and the Barents Sea area: ice sheet extent and configuration. *Quaternary Science Reviews 17*, 43–75.

Lien, R., Solheim, A., Elverhøi, A. & Rokoengen, K. 1989: Iceberg scouring and sea bed morphology on the eastern Weddell Sea shelf, Antarctica. *Polar Research 7*, 43–57.

Livingstone, S. J., Cofaigh, C. Ó., Stokes, C. R., Hillenbrand, C.-D., Vieli, A. & Jamieson, S. S. R. 2013: Glacial geomorphology of Marguerite Bay Palaeo-Ice stream, western Antarctic Peninsula. *Journal of Maps 9*, 558–572.

Llopart, J., Urgeles, R., Camerlenghi, A., Lucchi, R. G., Rebesco, M. & De Mol, B. 2015: Late Quaternary development of the Storfjorden and Kveithola Trough Mouth Fans, northwestern Barents Sea. *Quaternary Science Reviews 129*, 68–84.

Lucchi, R. G., Camerlenghi, A., Rebesco, M., Colmenero-Hidalgo, E., Sierro, F. J., Sagnotti, L., Urgeles, R., Melis, R., Morigi, C., Barcena, M. A., Giorgetti, G., Villa, G., Persico, D., Flores, J. A., Rigual-Hernandez, A. S., Pedrosa, M. T., Macri, P. & Caburlotto, A. 2013: Postglacial sedimentary processes on the Storfjorden and Kveithola trough mouth fans: significance of extreme glacimarine sedimentation. *Global and Planetary Change 111*, 309–326.

Lucchi, R. G., Pedrosa, M. T., Camerlenghi, A., Urgeles, R., De Mol, B. & Rebesco, M. 2012: Recent Submarine Landslides on the Continental Slope of Storfjorden and Kveithola Trough-Mouth Fans (North West Barents Sea). *In* Yamada, Y., Kawamura, K., Ikehara, K., Ogawa, Y., Urgeles, R., Mosher, D., Chaytor, J. & Strasser, M. (eds.): *Submarine Mass Movements and Their Consequences. Advances in Natural and Technological Hazards Research*, 735–745. Springer Science Book Series 31, Dordrecht.

MacLean, B., Blasco, S., Bennett, R., England, J., Rainey, W., Hughes-Clarke, J. & Beaudoin, J. 2010: Ice keel seabed features in marine channels of the central Canadian Arctic Archipelago: evidence for former ice streams and iceberg scouring. *Quaternary Science Reviews 29*, 2280–2301.

Mangerud, J., Bondevik, S., Gulliksen, S., Karin Hufthammer, A. & Høistæter, T. 2006: Marine 14C reservoir ages for 19th century whales and molluscs from the north Atlantic. *Quaternary Science Reviews 25*, 3228–3245.

Moon, T. & Joughin, I. 2008: Changes in ice front position on Greenland's outlet glaciers from 1992 to 2007. *Journal of Geophysical Research 113*, F02022. https://doi.org/10.1029/2007JF000927.

Motyka, R. J., Hunter, L., Echelmeyer, K. A. & Connor, C. 2003: Submarine melting at the terminus of a temperate tidewater glacier, LeConte Glacier, Alaska, U.S.A. *Annals of Glaciology 36*, 57–65.

Motyka, R. J., Truffer, M., Fahnestock, M., Mortensen, J., Rysgaard, S. & Howat, I. 2011: Submarine melting of the 1985 Jakobshavn Isbræ floating tongue and the triggering of the current retreat. *Journal of Geophysical Research: Earth Surface 116*, F01007. https://doi.org/10.1029/2009JF001632.

Nick, F. M., Vieli, A., Howat, I. M. & Joughin, I. 2009: Large-scale changes in Greenland outlet glacier dynamics triggered at the terminus. *Nature Geoscience 2*, 110–114.

Nielsen, T. & Rasmussen, T. L. 2018: Reconstruction of ice sheet retreat after the Last Glacial maximum in Storfjorden, southern Svalbard. *Marine Geology 402*, 228–243.

Ottesen, D. & Dowdeswell, J. A. 2006: Assemblages of submarine landforms produced by tidewater glaciers in Svalbard. *Journal of Geophysical Research: Earth Surface 111*, F01016, https://doi.org/10.1029/2005JF000330

Ottesen, D., Dowdeswell, J. A. & Rise, L. 2005: Submarine landforms and the reconstruction of fast-flowing ice streams within a large Quaternary ice sheet: the 2500-km-long Norwegian-Svalbard margin (57-80N). *Bulletin of the Geological Society of America 117*, 1033–1050.

Ottesen, D., Stokes, C. R., Rise, L. & Olsen, L. 2008: Ice-sheet dynamics and ice streaming along the coastal parts of northern Norway. *Quaternary Science Reviews 27*, 922–940.

Patton, H., Andreassen, K., Bjarnadóttir, L. R., Dowdeswell, J. A., Winsborrow, M. C. M., Noormets, R., Polyak, L., Auriac, A. & Hubbard, A. 2015: Geophysical constraints on the dynamics and retreat of the Barents Sea Ice Sheet as a palaeo-benchmark for models of marine ice-sheet deglaciation. *Reviews of Geophysics 53*, 1051–1098.

Patton, H., Hubbard, A., Andreassen, K., Auriac, A., Whitehouse, P. L., Stroeven, A. P., Shackleton, C., Winsborrow, M. C. M., Heyman, J. & Hall, A. M. 2017: Deglaciation of the Eurasian ice sheet complex. *Quaternary Science Reviews 169*, 148–172.

Pattyn, F., Huyghe, A., De Brabander, S. & De Smedt, B. 2006: Role of transition zones in marine ice sheet dynamics. *Journal of Geophysical Research: Earth Surface 111*, F02004, https://doi.org/10.1029/2005JF000394.

Pedrosa, M. T., Camerlenghi, A., De Mol, B., Urgeles, R., Rebesco, M. & Lucchi, R. G. 2011: Seabed morphology and shallow sedimentary structure of the Storfjorden and Kveithola trough-mouth fans (North West Barents Sea). *Marine Geology 286*, 65–81.

Peltier, W. R. & Fairbanks, R. G. 2006: Global glacial ice volume and Last Glacial Maximum duration from an extended Barbados sea level record. *Quaternary Science Reviews 25*, 3322–3337.

Powell, R. D. 1990: Glacimarine processes at grounding-line fans and their growth to ice-contact deltas. *Geological Society, London, Special Publications 53*, 53–73.

Powell, R. D. & Alley, R. B. 1997: Grounding-line systems: Processes, glaciological inferences and the stratigraphic record. Geology and Seismic Stratigraphy of the Antarctic Margin, Part 2. *Antarctic Research Series 71*, 169–187.

Powell, R. D. & Domack, E. 2002: Modern glaciomarine environments. *In* Menzies, J. (ed.): *Modern and Past Glacial Environments*, 361–389. Butterworth-Heinmann, Oxford.

Powell, R. D. & Molnia, B. 1989: Glacimarine sedimentary processes, facies and morphology of the south-southeast Alaska shelf and fjords. *Marine Geology 85*, 359–390.

Powell, R. D., Dawber, M., McInnes, J. N. & Pyne, A. R. 1996: Observations of the grounding-line area at a floating glacier terminus. *Annals of Glaciology 22*, 217–223.

Pritchard, H. D., Arthern, R. J., Vaughan, D. G. & Edwards, L. A. 2009: Extensive dynamic thinning on the margins of the Greenland and Antarctic ice sheets. *Nature 461*, 971–975.

Rasmussen, T. L. & Thomsen, E. 2014: Brine formation in relation to climate changes and ice retreat during the last 15,000 years in Storfjorden, Svalbard, 76-78°N. *Paleoceanography 29*, 911–929.

Rasmussen, T. L., Thomsen, E., Ślubowska, M. A., Jessen, S., Solheim, A. & Koç, N. 2007: Paleoceanographic evolution of the SW Svalbard margin (76°N) since 20,000 ^{14}C yr BP. *Quaternary Research 67*, 100–114.

Rebesco, M., Liu, Y., Camerlenghi, A., Winsborrow, M. C. M., Sverre, J., Caburlotto, A., Diviacco, P., Accettella, D., Sauli, C., Wardell, N. & Tomini, I. 2011: Deglaciation of the western margin of the Barents Sea Ice Sheet — A swath bathymetric and sub-bottom seismic study from the Kveithola Trough. *Marine Geology 279*, 141–147.

Reimer, P. J., Bard, E., Bayliss, A., Beck, J. W., Blackwell, P. G., Ramsey, C. B., Buck, C. E., Cheng, H., Edwards, L., Friedrich, M., Grootes, P. M., Guilderson, T. P., Haflidason, H., Hajdas, I., Hatté, C., Heaton, T. J., Hoffmann, D. L., Hogg, A. G., Hughen, K. A., Kaiser, K. F., Kromer, B., Manning, S. W., Niu, M., Reimer, R. W., Richards, D. A., Scott, E. M., Southon, J. R., Staff, R. A., Turney, C. S. & van der Plicht, J. 2013: IntCal13 and Marine 13 radiocarbon age calibration curves 0-50,000 years cal BP. *Radiocarbon 55*, 1869–1887.

Rignot, E., Koppes, M. & Velicogna, I. 2010: Rapid submarine melting of the calving faces of West Greenland glaciers. *Nature Geoscience 3*, 187–191.

Rignot, E., Mouginot, J. & Scheuchl, B. 2011: Ice flow of the Antarctic ice sheet. *Science 333*, 1427–1430.

Schoof, C. 2007: Ice sheet grounding line dynamics: steady states, stability, and hysteresis. *Journal of Geophysical Research: Earth Surface 112*, F03S28, https://doi.org/10.1029/2006JF000664.

Serov, P., Vadakkepuliyambatta, S., Mienert, J., Patton, H., Portnov, A., Silyakova, A., Panieri, G., Carroll, M. L., Carroll, J., Andreassen, K. & Hubbard, A. 2017: Postglacial response of Arctic Ocean gas hydrates to climatic amelioration. *Proceedings of the National Academy of Sciences 114*, 6215–6220.

Shackleton, C., Patton, H., Hubbard, A., Winsborrow, M., Kingslake, J., Esteves, M., Andreassen, K. & Greenwood, S. L. 2018: Subglacial water storage and drainage beneath the Fennoscandian and Barents Sea ice sheets. *Quaternary Science Reviews 201*, 13–28.

Shreve, R. L. 1972: The movement of water in glaciers. *Journal of Glaciology 11*, 205–214.

Slater, D. A., Nienow, P. W., Cowton, T. R., Goldberg, D. N. & Sole, A. J. 2015: Effect of near-terminus subglacial hydrology on tidewater glacier submarine melt rates. *Geophysical Research Letters 42*, 2861–2868.

Smith, S. D. & Banke, E. G. 1983: The influence of winds, currents and towing forces on the drift of icebergs. *Cold Regions Science and Technology 6*, 241–255.

Sole, A., Payne, T., Bamber, J., Nienow, P. & Krabill, W. 2008: Testing hypotheses of the cause of peripheral thinning of the Greenland Ice Sheet: Is land-terminating ice thinning at anomalously high rates? *The Cryosphere 2*, 205–218.

Stokes, C. & Clark, C. 2001: Palaeo-ice streams. *Quaternary Science Reviews 20*, 1437–1457.

Stuiver, M. & Reimer, P. J. 1993: Extended ^{14}C database and revised CALIB 3.0 ^{14}C age calibration program. *Radiocarbon 35*, 215–230.

Syvitski, J. P. M. 1989: On the deposition of sediment within glacier-influenced fjords: oceanographic controls. *Marine Geology 85*, 301–329.

Thomas, R. H. 1979: The dynamics of marine ice sheets. *Journal of Glaciology 24*, 167–177.

Vorren, T. O. & Laberg, J. S. 1997: Trough mouth fans — palaeoclimate and ice-sheet monitors. *Quaternary Science Reviews 16*, 865–881.

Wise, M. G., Dowdeswell, J. A., Jakobsson, M. & Larter, R. D. 2017: Evidence of marine ice-cliff instability in Pine Island Bay from iceberg-keel plough marks. *Nature 550*, 506–510.